Relation between nonequilibrium Green's function and Lippmann-Schwinger formalism in the first-principles quantum transport theory

Jian Wang*
Department of Physics and The Center of Theoretical and Computational Physics, The University of Hong Kong, Pokfulam Road, Hong Kong, China

Hong Guo
Department of Physics, McGill University, Montreal, Quebec, Canada H3A 2T8

(Received 7 August 2008; revised manuscript received 9 December 2008; published 23 January 2009)

In first-principles theory of *nonequilibrium* quantum transport, there are two main formalisms—the nonequilibrium Green's function (NEGF) and the Lippmann-Schwinger (LS) equation, which have been applied to a wide range of device physics problems when coupled with electronic structure methods such as the density-functional theory. In this work, we derive a relationship that formally connects the two formalisms at nonequilibrium. The relation is between the *nonequilibrium* scattering wave function and NEGF and it *cannot* be derived directly from the LS equation itself. We also found that the relation is practically useful by giving rise to a significant speed up in numerical computation of transmission coefficients for multiprobe systems.

DOI: 10.1103/PhysRevB.79.045119 PACS number(s): 72.10.Bg, 73.63.−b, 73.23.−b

I. INTRODUCTION

Quantitative theory of nonlinear and nonequilibrium quantum transport of nanoelectronic devices is important not only for understanding quantum device physics but also for practical applications in technology. At truly nanoscale, electron and spin transport are critically influenced by atomic, chemical, and materials properties of the device, as well as by nonequilibrium statistical properties of the device scattering region when bias voltage is applied and charge or spin current flows. A quantitative theory should therefore calculate the device Hamiltonian H under nonequilibrium transport conditions from atomic first principles. In order to handle large number of atoms while keeping reasonable accuracy, state-of-the-art and practical nanodevice modeling techniques are all based on density-functional theory (DFT) for calculating H.[1–17] In addition, the nonequilibrium transport conditions under finite bias are treated by either the Keldysh nonequilibrium Green's functions (NEGF) (Ref. 3) or by filling electronic levels of H according to the chemical potentials of different device leads.[1] Mathematically, the former is the matrix Green's function-based technique while the latter is a scattering wave-function-based technique where a particularly powerful implementation is by using the Lippmann-Schwinger (LS) equation.[1]

So far, both NEGF-DFT and LS-DFT methods have been applied to a wide range of problems of quantum transport in nanoelectronics. While these two formalisms are expected to have a formal connection at *nonequilibrium*, to the best of our knowledge such a connection has yet to be found. We recall, for example, the well-known Fisher-Lee relation[18] which connects *scattering matrix* to the Green's functions at the boundary of the device scattering region. Another example is the injectivity that relates scattering wave-function *density* $|\psi|^2$ inside the scattering region to the Green's function.[19] It is the purpose of this work to go one step further, namely, to establish a formal connection of NEGF and LS nonequilibrium transport formalisms. In particular, we derive a relation between the *nonequilibrium* scattering wave function and NEGF and this relation *cannot* be derived directly from the LS equation itself. We also found that this relation is practically useful by giving rise to a significant speed up in numerical computation of transmission coefficients for multiprobe systems; therefore it provides a different technique which is a hybridization of NEGF+DFT and LS+DFT.

II. THEORY AND NUMERICAL CALCULATIONS

We begin by briefly discussing the LS-DFT and NEGF-DFT formalisms. In LS-DFT, one solves the LS equation,[1]

$$|\psi_\alpha\rangle = |\psi_\alpha^0\rangle + G_0^r V|\psi_\alpha\rangle. \tag{1}$$

Here, the device Hamiltonian H is divided into two parts $H=H_0+V$ where V is the scattering potential including the self-consistent Coulomb interaction U; $G_0^r=1/(E-H_0+i\eta)$; ψ_α^0 is the scattering wave function from lead α at $V=0$. Here $|\psi_\alpha\rangle$ and $|\psi_\alpha^0\rangle$ are wave functions of the infinite system including the lead regions. If one restricts the wave functions in the scattering region, a self-energy Σ^r has to be included to account for the external leads and LS equation is still given by Eq. (1) but with $G_0^r=1/(E-H_0-\Sigma^r)$. The Coulomb potential U is obtained from the Poisson equation subjected to proper device boundary conditions,

$$\nabla^2 U = -4\pi\rho(\mathbf{r}). \tag{2}$$

The real-space-charge density $\rho(\mathbf{r})$ is contributed by both left- and right-coming scattering wave functions as well as by bound states of the open device system, and Eqs. (1) and (2) are iterated to self-consistency.[1] In the pioneering paper of Lang,[1] the Green's function G_0^r of Eq. (1) is written analytically due to the use of jellium model for the device leads: this approximation drastically reduces complexity of the calculations. It is often necessary to use full atomic structures to realistically model devices leads which is so far an unsolved problem within LS-DFT.

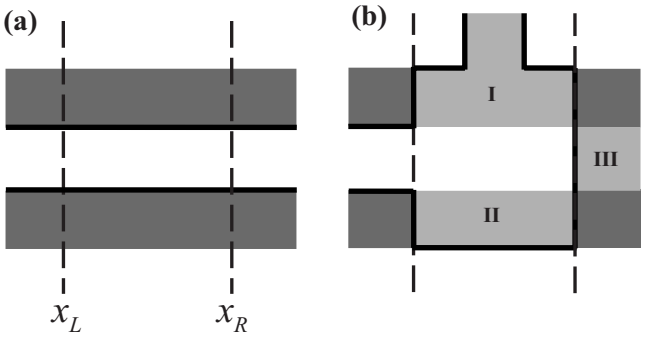

FIG. 1. (a) A two-probe nanostructure where exact solutions of the scattering wave function; the linewidth function Γ and NEGF are available. (b) An arbitrary two-probe nanostructure after adding a potential V_2 inside the scattering region.

In the NEGF-DFT formalism,[3] the device is divided into three parts: left or right leads plus the scattering region, as shown in Fig. 1. The retarded Green's function of the scattering region is calculated by direct matrix inversion,

$$G^r = \frac{1}{E - H - \Sigma^r}, \tag{3}$$

where Σ^r is the self-energy due to the presence of atomic leads; H is the Hamiltonian of the device scattering region that includes the self-consistent Coulomb potential U determined by Eq. (2) as well as other interactions such as the exchange-correlation potential $V_{\rm xc}[\rho]$. In NEGF-DFT, the charge-density matrix ρ is obtained from the distribution function $G^<$ which in turn is related to the retarded Green's function G^r through the Keldysh equation.[3,20] By solving Eqs. (3) and (2) and $G^<$ to self-consistency, the Hamiltonian H, NEGF, and hence all the scattering properties are obtained from atomic first principles. So far, the NEGF-DFT formalism has been implemented by many groups[3–6,8–13,16,17] and applied to large number quantum transport problems.

We now proceed to derive a formal connection between wave-function-based approach (LS-DFT) to the Green's function-based approach (NEGF-DFT). For transport problems, there are three possible wave functions for an electron with energy E: scattering states $|\psi_{L/R}\rangle$ for which electrons come from the left (L) or right (R) lead and bound state $|\psi_b\rangle$ which lives inside the scattering region. Hence in general we can write the density matrix[3] of the scattering region as

$$\hat{\rho}(E) = \sum_{\alpha m} \frac{1}{h v_m} |\psi_{\alpha m}\rangle\langle\psi_{\alpha m}| f_\alpha(E) + \sum_b f(E)\,\delta(E - E_b)|\psi_b\rangle\langle\psi_b|, \tag{4}$$

where $f_\alpha \equiv f(E - q v_\alpha)$ is the Fermi distribution function and $\alpha = L, R$, $|\psi_{Lm}\rangle$ is the scattering wave-function for incident electrons coming from left lead on quantum channel m and v_m is the channel's group velocity. Next, we wish to derive the same equation of density matrix using NEGF. In the NEGF formalism, the density matrix of the scattering region is given by $\hat{\rho} = -iG^</(2\pi)$ where $G^<$ satisfies the Keldysh equation,

$$G^< = (1 + G^r\Sigma^r)G_0^<(1 + \Sigma^a G^a) + G^r\Sigma^< G^a, \tag{5}$$

here $\Sigma^< = i\Sigma_\alpha \Gamma_\alpha f_\alpha$ and Γ_α is the linewidth function of the device leads and $-iG_0^< = if(E)(G^{r0} - G^{a0})$ is the distribution function of the scattering region without the leads; G^{r0} is the retarded Green's function for the corresponding isolated system.

The first term of Eq. (5) actually vanishes except at discrete energies $E = E_b$ where E_b is the bound-state energy of the scattering region. This can be easily seen by considering a simple case where the scattering region has a single energy level E_0 so that $G^{r0} = 1/(E - E_0 + i\gamma)$ with $\gamma \to 0$. From Dyson equation $G^r = (1 + G^r\Sigma^r)G^{r0}$, the first term of Eq. (5) becomes

$$\mathbf{G}^r(G^{r0})^{-1}G_0^<(G^{a0})^{-1}\mathbf{G}^a = -f(E)\mathbf{G}^r[(G^{a0})^{-1} - (G^{r0})^{-1}]\mathbf{G}^a. \tag{6}$$

Because $(G^{a0})^{-1} - (G^{r0})^{-1} = -2i\gamma$ and $\gamma \to 0$, expression (6) vanishes at all energies except those of bound states E_b where $\mathbf{G}^{r,a}$ in the above expression diverges. The bound-states energies E_b can be found by setting the denominator of Eq. (3) to zero: $E - H - \Sigma^r(E_b) = E - H - \Sigma^a(E_b) = 0$. This is typically a highly nonlinear algebraic equation because all quantities are matrices. We now reduce the first term of Eq. (5) in terms of these bound states of the scattering region. Using the fact

$$(\mathbf{G}^r)^{-1} - (\mathbf{G}^a)^{-1} = (\mathbf{G}^{r0})^{-1} - (\mathbf{G}^{a0})^{-1},$$

expression (6) becomes $-f(E_b)[G^r(E_b) - G^a(E_b)] = 2\pi i \Sigma_b f(E)\,\delta(E - E_b)|\psi_b\rangle\langle\psi_b|$ by using the spectral form of the Green's functions in terms of the bound states which can be evaluated after E_b is found. For energies below the continuous spectrum of the scattering region, G^r of Eq. (3) can be written in the spectral form in terms of bound states,

$$G^r = \sum_b |\psi_b\rangle\langle\psi_b|/(E - E_b + i\gamma), \tag{7}$$

where $|\psi_b\rangle$ is the wave function of the bound states. Using the Plemelj formula $1/(z \pm i0^+) = P(1/z) \mp i\pi\delta(z)$, the first term of the Keldysh equation (5), i.e., expression (6), is reduced to $2i\pi\Sigma_b f(E)\,\delta(E - E_b)|\psi_b\rangle\langle\psi_b|$. Therefore, the density matrix of the scattering region in terms of NEGF can now be written as

$$\hat{\rho}(E) = \frac{-i}{2\pi}G^< = \sum_\alpha G^r\Gamma_\alpha G^a f_\alpha/(2\pi) + \sum_b f(E)\,\delta(E - E_b)|\psi_b\rangle\langle\psi_b|. \tag{8}$$

Comparing Eq. (8) to Eq. (4) suggests the following relation (to be proved below):

$$|\psi_{\alpha m}\rangle = \kappa_m G^r|W_{\alpha m}\rangle, \tag{9}$$

where $|W_{\alpha m}\rangle$ is the mth renormalized eigenstate of linewidth function matrix Γ_α such that $\Gamma_\alpha = \Sigma_m |W_{\alpha m}\rangle\langle W_{\alpha m}|$. The channel number m depends on the energy of incident electron, $\kappa_m = \sqrt{\hbar v_m}$, and v_m is the channel group velocity. Inverting Eq. (9), we obtain,

$$(E - H - \Sigma^r)|\psi_{\alpha m}\rangle = \kappa_m |W_{\alpha m}\rangle, \tag{10}$$

$$(E - H - \Sigma^r)|\psi_b\rangle = (E - H - \Sigma^a)|\psi_b\rangle = 0. \quad (11)$$

Here for completeness, we have also written down the equation for determining bound states ψ_b. Equations (9)–(11) are the central results of this paper: they connect scattering wave function $|\psi_{\alpha m}\rangle$ in the scattering region to the corresponding Green's function G^r. Furthermore, we will show below that they provide the formal connection between LS and the NEGF transport formalisms.

To prove Eq. (10), we start by considering a two-dimensional (2D) two-probe quantum nanostructure shown in Fig. 1(a) where the confining potential $V_1 = V_0$ is nonzero in the gray area. For simplicity, let us assume a hard wall confinement $V_0 = \infty$. Once Eq. (10) is proved for this simple geometry, we can then prove it for any arbitrary geometry using the LS equation. For the system in Fig. 1(a), the Green's function has been calculated before,[20]

$$G^r(x,y,x',y') = \sum_m \frac{-i}{\hbar v_m}\chi_m(y)\chi_m(y')\exp[ik_m|x-x'|], \quad (12)$$

where $k_m = \sqrt{2m(E-\epsilon_m)}/\hbar$ with ϵ_m as the threshold of quantum channel m and $v_m = \hbar k_m/m$. Here χ_m is the normalized transverse-mode wave function. The linewidth function is given by[20]

$$\Gamma_\alpha(x,y,x',y') = \sum_m \chi_m(y)\hbar v_m \chi_m(y')\,\delta(x-x_\alpha)\,\delta(x-x'), \quad (13)$$

where x_α is the x coordinate of the interface between scattering region and the lead α [indicated by vertical dash lines in Fig. 1(a)]. For this system, the scattering wave function is simply[20] $|\psi_{L/R}\rangle = \chi_m(y)\exp[\pm ik_m x]$ after choosing the origin of the coordinates such that $x_\alpha = 0$.

Now we prove Eq. (10) gives the same wave function $|\psi_{L/R}\rangle$. From the above linewidth function $\Gamma_\alpha(x,y,x',y')$, it is not difficult to obtain the W function $|W_{\alpha m}\rangle$ used in Eq. (9),

$$W_{\alpha m}(x,y) = \kappa_m \chi_m(y)\,\delta(x-x_\alpha). \quad (14)$$

Therefore from Eq. (10), the scattering wave function is

$$\psi_{\alpha m}(x,y) = \kappa_m \int dx'dy' G^r(x,y,x',y') W_{\alpha m}(x',y') = -i\chi_m(y)\exp[ik_m|x-x_\alpha|]. \quad (15)$$

Since $x_L \le x \le x_R$, we have

$$|\psi_{L/Rm}\rangle = \chi_m(y)\exp[\pm ik_m x + ik_m|x_{L/R}| - i\pi/2],$$

which are the same wave functions as quoted above since the factor $\exp[ik_m|x_\alpha|]$ is unity by adopting the same coordinate system used in Ref. 20 (i.e., $x_\alpha = 0$). Now the physical meaning of the wave function in Eq. (10) becomes clear: $|\psi_{\alpha m}\rangle$ is precisely the scattering wave function in the scattering region with the origin chosen at the interface between the scattering region and the lead α, i.e., setting $x_\alpha = 0$.

Having proved Eq. (10) for the simple structure of Fig. 1(a), we now prove it for an arbitrary geometry shown in Fig. 1(b). Compare with that in Fig. 1(a), the potential in the scattering region of Fig. 1(b) can be viewed as modified to $V = V_1 + V_2$ with $V_2 = -V_0$ in regions I and II and $V_2 = V_0$ in region III. Then, using the LS equation with $G_0^r = 1/(E - H_0 - \Sigma^r)$, Eq. (1) becomes

$$|\psi_{\alpha m}\rangle = \kappa_m G_0^r |W_{\alpha m}\rangle + G_0^r V_2 |\psi_{\alpha m}\rangle.$$

From this equation, solving for $|\psi_{\alpha m}\rangle$ we indeed obtain Eq. (9) with $G^r = 1/([G_0^r]^{-1} - V_2 - \Sigma^r)$. Finally, when the potential in the scattering region is not constant, Eq. (10) can be proved in a similar fashion. In addition, it is also straightforward to prove Eq. (10) when magnetic field is present.

It is easy to see that the LS equation follows from Eq. (10). From the Dyson equation $G^r = G_0^r + G_0^r V_2 G^r$, multiplying both sides by $|W_{\alpha m}\rangle$, we obtain

$$G^r|W_{\alpha m}\rangle = G_0^r|W_{\alpha m}\rangle + G_0^r V_2 G^r|W_{\alpha m}\rangle,$$

which is precisely the LS equation when Eq. (10) is used.[21] From the above discussion, we see that the result (10) is not equivalent to the LS equation in the sense that one cannot directly prove Eq. (10) from the LS equation [one has to first complete the proof for Fig. 1(a)]. Another interesting outcome of Eq. (9) is that the well-known Fisher-Lee relation between scattering matrix and the Green's function can be written in terms of the W function,

$$s_{\alpha\beta mn} = -\delta_{\alpha\beta mn} + i\langle W_{\alpha m}|G^r|W_{\beta n}\rangle = -\delta_{\alpha\beta mn} + i\langle W_{\alpha m}|\psi_{\beta n}\rangle/\kappa_m, \quad (16)$$

where $s_{\alpha\beta mn}$ is the scattering matrix element describing scattering event of channel n in lead β to channel m in lead α.

Having established the formal connection between LS and NEGF, we realize that Eq. (10) can be quite useful in DFT atomistic calculations of quantum transport, in addition to the existing NEGF-DFT (Ref. 3) and LS-DFT techniques.[1] First of all, when linear combination of atomic-orbital basis (LCAO) is used in DFT,[3–6,8–13,16,17] the matrix $E - H - \Sigma^r$ is in general a sparse matrix with a narrow bandwidth[3] for which an iterative numerical scheme for solving Eq. (10) becomes very efficient both computationally and storage wise. In contrast, in the LS (1), the factor $G_0^r V$ is not a sparse matrix hence it does not enjoy fast iterative numerics.

Secondly, even without using iterative scheme, solving the linear Eq. (10) is much faster and requires less memory than inverting a matrix to find the Green's function as in Eq. (3). Usually, the transfer-matrix method[22] is much faster than the matrix inversion. Note that the transfer-matrix method works well for the short-range overlap integral. For *ab initio* calculations, the overlap integral is of long range and the transfer-matrix method is not as fast unless one is interested in transport through a long nanowire. In addition, the transfer-matrix method is most suitable for a two-probe system when two leads are along the same direction [see Fig. 1(a)]. For multilead system or two-probe system when two leads are not along the same direction [see Fig. 1(b)], one has to use a modified transfer-matrix method (see Ref. 23). For the case of Fig. 1(a), our method has no advantage over transfer-matrix method for a long wire. For a multiprobe system or the case of Fig. 1(b), due to the long-range overlap integral the modified transfer-matrix method is very ineffi-

TABLE I. The CPU time for calculating transmission coefficient of several systems. The column labeled "direct inversion" indicates cost of CPU time by calculating Eq. (3). The last column is by calculating Eq. (10). The speed-up factor is significant across the board.

		Matrix size	Square ratio	Direct inversion	Our method
Molecular device	(22,0) CNT	2496	0.125	55.4s	6.57s
		4608	0.539	315.9s	10.74s
		Matrix size	Square ratio	Transfer matrix	Our method
Mesoscopic device	Square lattice	2116	0.0024	104s	37.5s
		4096	0.0013	308s	86.6s

cient. In this case our method is much faster.[24] For instance, if dimension of the matrix $E-H-\Sigma^r$ for a molecular device is around 2000, the speed gained by solving Eq. (10) over inverting this matrix to find the Green's function is a factor of 8 (see Table I).

Thirdly, when constructing the nonequilibrium part of the charge density, using Eqs. (9) and (4) is much faster than using Eq. (8) because the latter involves matrix multiplication $G^r\Sigma^< G^a$.[25] We note that our scheme (10) does involve a matrix diagonalization of Γ_α to find $|W_{\alpha m}\rangle$. However, the dimension of the matrix Γ_α is much smaller[3] than that of H since Γ_α represents the surface coupling: only those atoms near the lead-scattering region contribute to Γ_α. In addition, for a given electron energy, there usually exist only a few propagating eigenmodes on the order of ten. Hence one can use iterative methods, such as the Lanczos method, to quickly find these eigenmodes: this is possible because Γ_α is a symmetric positive-definite matrix. Significantly, although Eq. (10) has to be solved at each iteration step of the DFT self-consistent cycle, the diagonalization of Γ_α needs to be done only once for each energy.

We note in passing that Eq. (10) also provides an efficient technique for calculating transport properties of *mesoscopic* systems with multileads. Comparing with existing techniques for calculating transmission coefficient, Eq. (10) has very distinct advantages. It is much faster when applied to multiprobe systems or to two-probe systems where the two leads orient in different directions [e.g., Fig. 1(b)]; the construction of Hamiltonian is much simpler than that of the modified transfer-matrix method which has seen powerful applications in literature[23] and, similar to DFT transport calculations, devices with long-range coupling between distant sites can be easily handled.

To demonstrate the usefulness of our scheme Eq. (10), Table I tabulates the CPU time needed for calculating transmission coefficients for various systems. First, a (22,0) carbon nanotube (CNT) junction coupled to three leads was considered. For the direct matrix inversion method, the CPU time is solely determined by the dimension of the matrix in the denominator of Eq. (3). On the other hand, in our scheme (10), the CPU time is determined by the sparseness of the matrix as well as the dimension of the linewidth matrix Γ_α. The CPU time of using the scheme of Eq. (10) is roughly the same whether or not the orientation of the two devices leads is in the same direction. As another test, we consider a two-probe *mesoscopic* structures shown in Fig. 1(b) in the presence of disorder inside the scattering region and calculated transmission coefficients for 1000 disorder configurations using a tight-binding square lattice model. The reduction in CPU time is significant using our scheme (10) over a very fast modified transfer-matrix technique,[23] as shown in the last two rows of Table I. Finally, for all cases we examined, the speed-up factor increases as the system size grows.

III. SUMMARY

In summary, we have derived a relation between the nonequilibrium scattering wave function and the real-space Green's function (9). This relation formally connects the NEGF with the LS formalism at nonequilibrium but is, of course, valid at equilibrium as well. Importantly, Eqs. (9) and (10) cannot be directly derived from LS equation. Numerical investigations on various atomic junctions and mesoscopic systems indicate that relations (9) and (10) have very useful applications in quantum transport analysis; in particular it gives significant speed up over NEGF and LS methods for calculating transmission coefficients for multiprobe systems. Even compared with the best numerical scheme available in the mesoscopics literature, our scheme based on Eqs. (9) and (10) gives significant improvement in computational time.

ACKNOWLEDGMENTS

We gratefully acknowledge support by a RGC grant from the SAR Government of Hong Kong under Grant No. HKU 704607P. H.G. was supported by NSERC of Canada, FQRNT of Québec, and CIAR.

*jianwang@hkusub.hku.hk

[1] N. D. Lang, Phys. Rev. B **52**, 5335 (1995).
[2] K. Hirose and M. Tsukada, Phys. Rev. B **51**, 5278 (1995).
[3] J. Taylor, H. Guo, and J. Wang, Phys. Rev. B **63**, 245407 (2001); **63**, 121104 (2001).
[4] M. Brandbyge, J. L. Mozos, P. Ordejon, J. Taylor, and K. Stokbro, Phys. Rev. B **65**, 165401 (2002).
[5] Y. Xue, S. Datta, and M. A. Ratner, Chem. Phys. **281**, 151 (2002).
[6] J. J. Palacios, A. J. Perez-Jimenez, E. Louis, E. SanFabian, and J. A. Verges, Phys. Rev. B **66**, 035322 (2002); E. Louis, J. A. Verges, J. J. Palacios, A. J. Perez-Jimenez, and E. SanFabian, *ibid.* **67**, 155321 (2003).
[7] D. Wortmann, H. Ishida, and S. Blugel, Phys. Rev. B **66**, 075113 (2002).
[8] S.-H. Ke, H. U. Baranger, and W. T. Yang, Phys. Rev. B **70**, 085410 (2004).
[9] S. V. Faleev, F. Leonard, D. A. Stewart, and M. van Schilfgaarde, Phys. Rev. B **71**, 195422 (2005).
[10] Y. Asari, J. Nara, N. Kobayashi, and T. Ohno, Phys. Rev. B **72**, 035459 (2005).
[11] W. Lu, V. Meunier, and J. Bernholc, Phys. Rev. Lett. **95**, 206805 (2005).
[12] A. R. Rocha, V. M. Garcia-Suarez, S. Bailey, C. Lambert, J. Ferrer, and S. Sanvito, Phys. Rev. B **73**, 085414 (2006).
[13] D. Waldron, P. Haney, B. Larade, A. MacDonald, and H. Guo, Phys. Rev. Lett. **96**, 166804 (2006).
[14] K. Carva, I. Turek, J. Kudrnovsky, and O. Bengone, Phys. Rev. B **73**, 144421 (2006).
[15] P. Darancet, A. Ferretti, D. Mayou, and V. Olevano, Phys. Rev. B **75**, 075102 (2007).
[16] K. S. Thygesen and A. Rubio, Phys. Rev. B **77**, 115333 (2008).
[17] Y. Ke, K. Xia, and H. Guo, Phys. Rev. Lett. **100**, 166805 (2008).
[18] D. S. Fisher and P. A. Lee, Phys. Rev. B **23**, 6851 (1981).
[19] T. Gramespacher and M. Buttiker, Phys. Rev. B **56**, 13026 (1997).
[20] S. Datta, *Electronic Transport in Mesoscopic Systems* (Cambridge University Press, New York, 1995), pp. 137–148.
[21] When the device lead is a periodic atomic structure (not jellium), the scattering wave function is a Bloch wave $\psi_{L/R} = u_{k_m,m}(x,y)\exp[\pm ik_m x]$. The proof can be carried out similarly by replacing $\chi_m(y)$ in Eqs. (12)–(14) with $u_{k_m,m}(x,y)$.
[22] T. Markussen, R. Rurali, M. Brandbyge, and A. P. Jauho, Phys. Rev. B **74**, 245313 (2006).
[23] Z. H. Qiao and J. Wang, Nanotechnology **18**, 435402 (2007).
[24] We wish to mention that one of the reasons for speed up is due to LU matrix factorization using UMFPACK method for a sparse matrix (available in Matlab).
[25] For the calculation of charge density, the speed up of our scheme comes from two sources: (1) Suppose G^r is a $N \times N$ matrix and Γ_α is a $N_1 \times N_1$ matrix with N_1 much smaller than N. The charge density is given by the diagonal matrix elements of $G^r \Gamma G^a$ with the number of operations $2NN_1(N_1+1)$. Note that the dimension of $|W_\alpha\rangle$ is $N_1 \times N_2$ where N_2 is the number of propagating channels that is much smaller than N_1. The number of operations using the scattering wave function from our scheme is $2NN_2(N_2+1)$. This is the first reason why there is a speed up. (2) Note that there are N^2 elements in the retarded Green's function. If one is only interested in transmission coefficient, it is enough to calculate only a subset of G^r with $N_3 \times N_3$ elements with N_3 ($N_3 \geq N_1$) is the number of sites or orbitals in the basic unit in the transfer-matrix method. In order to calculate the charge density, one has to calculate $2N \times N_3$ elements of G^r which requires more computer time. In the scattering wave-function calculation, however, no extra time is required other than multiplication of the matrix $N \times N_2$ by its transpose $N_2 \times N$ mentioned above to get $|\Psi|^2$. This is the second reason for the speed up. If one does not use the transfer-matrix method, then speed up is only due to Eq. (1).